XX IMEKO World Congress
Metrology for Green Growth
September 9–14, 2012, Busan, Republic of Korea

MEASUREMENT OF WALKING GAIT FOR 3D PASSIVE DYNAMIC BIPED WALKER

T. Ito[1], *T. Kinugasa*[1], *T. Akagi*[1], *S. Fujimoto*[1], *K. Yoshida*[1], *and M. Iribe*[2]

1: Okayama University of Science, Okayama, Japan, kinugasa@mech.ous.ac.jp
2: Osaka Electro-Communication University, Osaka, Japan

Abstract: Passive dynamic bipedal walking (PDW) is an attractive topic not only for robotics field but also the other scientific fields, i.e. physics and biology. In order to clarify its mechanism of walking, many researchers have developed various PDW machines. We also have developed several 3-D PDW with flat feet and ankle springs. However there are no researches on the measurement of 3-D PDW gait, which reveals its mechanism precisely. This paper, therefore, describes measurement of walking gait of 3-D PDW such as zero moment point (ZMP) and its posture which are often measured for human gait analysis. A unique flexible displacement sensor and a usual 6 axes force sensor are utilized for the measurement. As a result, ZMP trajectory draws '8' shape pattern, which is similar to that of human. Moreover the measurement system clarified the relationship between walking gait and ballast position which is effective for stabilization.

Keywords: Passive dynamic walking, gait measurement, flexible displacement sensor, zero moment point.

1. INTRODUCTION

For the last two decades, many researchers have been focused on passive dynamic walking (PDW) [1] because PDW is an essence of biped walking. PDW changes its gait in order to adapt to variation of its body configuration and environment, and has high energy efficiency. If you can develop a biped which can achieve PDW, then we can expect that the biped will provide better performance in the sense that its configuration is suitable for biped walking.

Almost all of the previous researches on PDW adopted circular arc or spherical soles so that their biped can walk stably. However contacting area between the sole and the ground is small, thus the area cannot provide enough friction force against yaw moment. Moreover, if the radius of the arc foot is small, then the biped cannot keep standing still. On the other hand, flat soles provide higher friction force against rotation about yaw axis and stable standing still posture easily. In addition, ankle springs is in stability similar to circular soles [2].

Based on the properties, we have developed some 3-D bipeds using the flat soles and the ankle springs and achieved stable gait [3, 4, 5]. Stability of 3-D walking gait contacting to a surface instead of a point or a line segment strongly relates to movement of Zero Moment Point (ZMP). It is well known that ZMP and the posture are measured for analysis of human gait. There are few researches on 3-D PDW [6] and similar 3-D bipeds using ballistic walking strategy [7, 8], however they have not measured its ZMP and posture because PDW is not so robust against variation of its configuration such as implementation of some additional devices. It is also important that the both information are measured in order to synthesize an active dynamic biped based on PDW.

The purpose of the paper, therefore, is to reveal fundamental property of three dimensional passive dynamic biped walking with flat soles and ankle springs. First, we develop a stable and relatively robust 3-D PDW called 'RW03' with flat soles and ankle springs. Next, some sensors are implemented in order to measure the posture and ZMP trajectory of our prototype. Finally, we investigate relationship between its gait and center of mass (CoM) position of each leg, which is effective for walking stability.

2. 3-D PASSIVE DYNAMIC WALKER 'RW03'

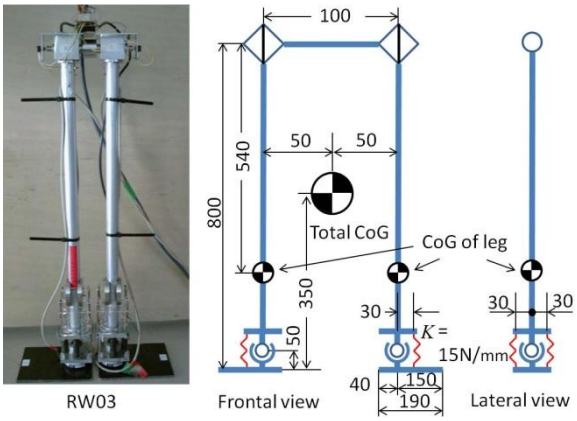

Fig.1 3-D passive dynamic walker 'RW03'

Fig.1 shows a photograph and a schematic of the walker called RW03. RW03 has two legs which has a foot and is connected each other by a coxa shaft. The both coxa angle can be measured by rotary potentiometers. Sole of the foot is flat and an ankle joint is composed of a ball joint and three coil springs attached on the front, the rear and the outside of the joint. A shaft is attached on the inside of the joint in order to keep the foot plate horizontal in swing phase. Stiffness of the coil spring is 15 N/mm. The design method

for the spring stiffness is denoted in [2, 4]. Aluminium disks as ballast (Fig.2) of which weight is 500 g is attached to each leg, which is adjusted so that the biped can walk stably [5].

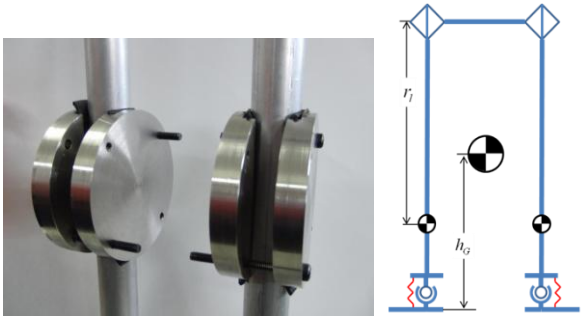

Fig.2 Ballasts (500 g) and CoG position

3. FUNDAMENTAL TEST

Firstly, walking distance, the number of total steps and stride are investigated using RW03 against variation of the ballast position and slope inclination. In the test, the coxa angle can be measured by the potentiometers. The total weight of RW03 is 4.18 kg. The slope on which RW03 walks is 3.6 m long and 0.9 m wide (Fig.3). Inclination angle of the slope can be changed. We repeat the test procedures 10 times for each condition. The ballast position is changed from 160 mm to 200 mm every 10 mm. As a result, the total CoM position h_G and the CoM position of one leg r_l are changed as shown in Table 1. The table also describes frequency of the leg and the lateral oscillation.


Fig. 3 Slope 3.6 m x 0.9 m

Table 1 Parameters of biped with respect to ballast position

Ballast[mm]	160	170	180	190	200
r_l [mm]	503	501	498	496	495
h_G [mm]	340	343	346	348	350
Leg freq. [rad/s]	3.77	3.76	3.78	3.77	3.80
Lateral freq. [rad/s]	5.22	4.91	4.88	4.95	4.96

Figure 4 shows walking distance vs. the ballast position against the slope variation normalized by the slope length and the leg length, respectively. Blue, green and red lines indicate the slope inclination 3.5, 4.0 and 4.5 degrees. Figure 5 indicates stride of walking normalized by the leg length. Though variation of the distance and the stride with respect to the ballast position is depending on the slope inclination, there is an optimal ballast position for each slope angle in the sense of walking distance.

Figure 6 shows walking distance normalized by the slope length against the slope inclination. The walking distance decreases when the slope angle increases, of which tendency is invariant against the ballast position.

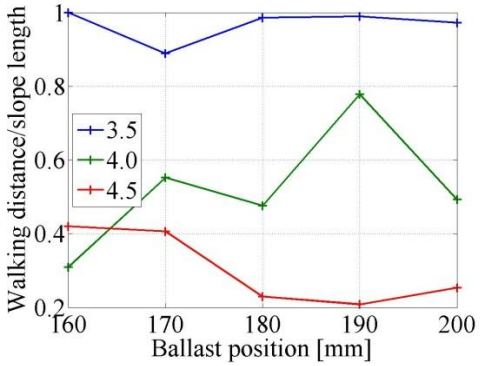

Fig.4 Walking distance vs. ballast position

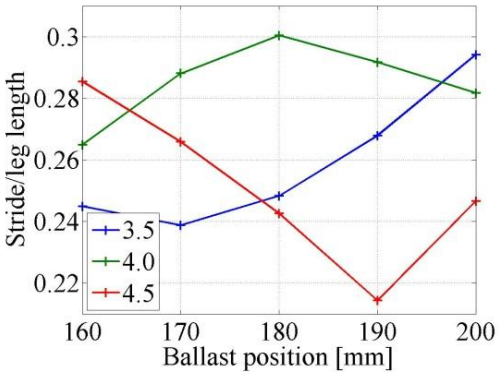

Fig.5 Stride vs. ballast position

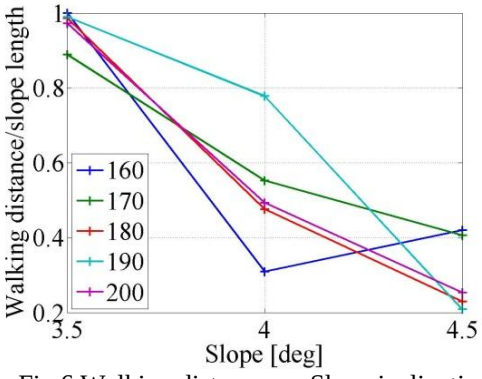

Fig.6 Walking distance vs. Slope inclination

4. MEASUREMENT OF WALKING GAIT

In order to measure the gait pattern and ZMP trajectory, some sensors mentioned below are implemented. As a result, the total weight of RW03 became 4.27 kg and a leg 1.8 kg.

4.1 Flexible Displacement Sensor and Posture of Walker

A choice of the measurement system for 3-D passive dynamic walking gait is a motion capture system. However, the motion capture systems, particularly for 3-D motion, are expensive and need a large space in order to place many video cameras. Suppose the sole of the stance foot is completely contacted to the ground, then the posture of the walker is decided by angles of stance leg ankle and coxa. Hence a unique sensor is introduced, in order to measure the angle of the ankle joint, which is called string type flexible displacement sensor developed by Hamamoto [9]. For the coxa angle, a usual rotary potentiometer is implemented.

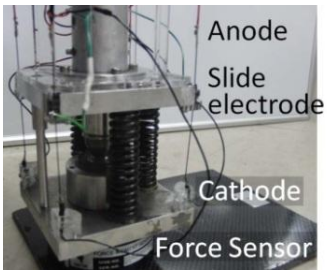

Fig.7 Ankle joint and flexible displacement sensors

Figure 7 shows the ankle joint. In the figure, a black line located at each corners of two square plates is a nylon string coated with carbon powder (NSCC) which roles as a flexible resistance. A slide electrode is embedded at each corner of the upper plate, and a fixed electrode (cathode) the lower one. The opposite end of NSCC is also a fixed electrode (anode), which is gently pulled by a rubber line. The attitude of the ankle joint is decided by three angles, roll, pitch and yaw. Since we expect that the yaw motion is enough small, the ankle can be expressed by two independent axes, direction angle θ and flexed angle α . Here we assume that NSCC flexes as an arc, then the both angles can derived by the following equations:

$$\theta = \tan^{-1}\frac{\Delta L_4 - \Delta L_2}{\Delta L_3 - \Delta L_1}$$

$$\alpha = \frac{\sqrt{(\Delta L_4 - \Delta L_2)^2 + (\Delta L_3 - \Delta L_1)^2}}{2r}$$

where, $\Delta L_n = \acute{L}_n - L_n$ (n = 1~4) is variation of each flexible sensor, and L_n (n = 1~4) is the initial length between the fixed electrode and the slide electrode and $\acute{L}_n$ (n = 1~4) is the length after deformation. For the ankle joint, the direction angle represents the direction where the leg inclines the most largely. The flexed angle is the angle of the inclination. Figure8 shows the schematic of the direction and flexed angles.

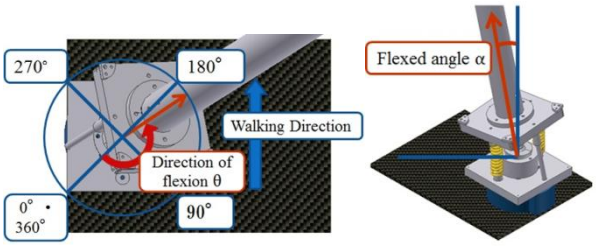

Fig.8 Schematic of direction and flexed angles

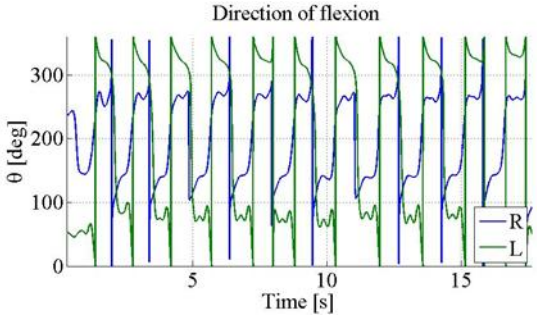

Fig.9 A time evolution of the direction angle θ

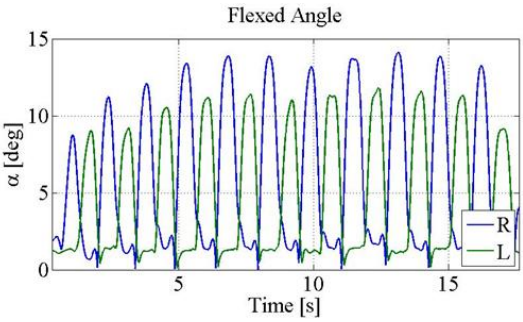

Fig.10 A time evolution of the flexed angle α

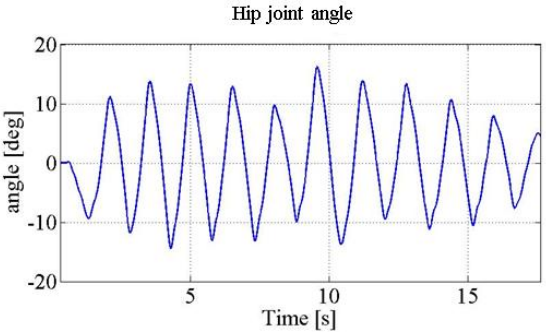

Fig.11 A time evolution of the coxa angle

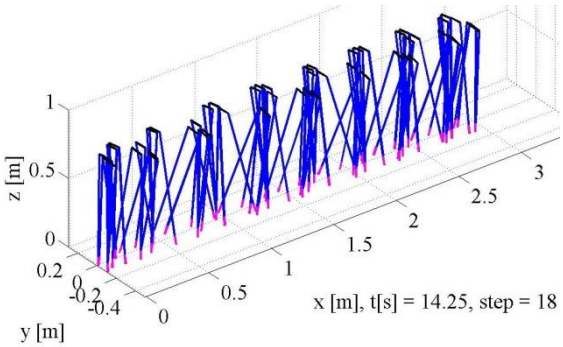

Fig.12 A gait pattern of RW03 measured by FDS

An example of walking tests are shown in Figs 9, 10 and 11 which represent the direction angle, flexed angle and the coxa angle, respectively. In the tests, the same slope as shown in Fig.3 is used and its inclination is 4.5 deg. The direction angle of the right leg (blue line of Fig.9) moves from 45 deg to 220 deg and stays around 270 deg. The direction from 45 to 220 is identical to the forward, the outside and the backward directions of the walker. At the same area, the flexed angle shown in Fig.10 yields a half wave pattern which means the stance phase. Peaks of the

flexed angle are occurred about 135 deg where the right hand side direction is identical. When the direction angle is staying around 270 deg, the right foot is leaving from the ground, that is, the swing phase.

Figure 12 depicted a gait pattern of RW03 by fusing the direction, flexed and coxa angles as shown in Figs 9 to 11. We can find that the walker walks in the positive direction of *x* axis with oscillation about roll axis. The oscillation is needed so that the swing foot can swing forward without scuffing

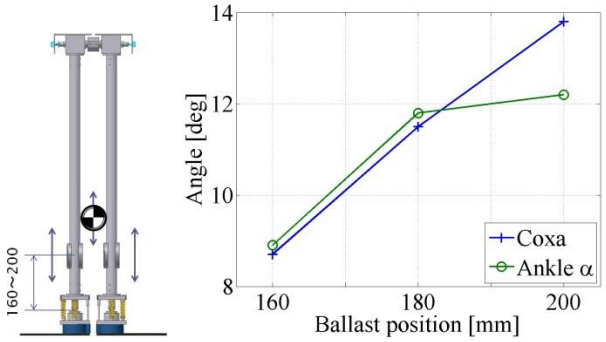

Fig.13 Ballast position vs. angle of coxa and ankle

Figure 13 shows magnitude of coxa angle and ankle angle versus ballast position. The ballast position is changed from 160 mm to 200 mm. CoG position is lower than that of the previous tests because of the additional sensors implementation. Magnitude of the both angles increase when the ballast position is elevated. It is difficult to keep walking when the magnitude of the oscillations is small, and biped will fall down when it is large. The ballast position, thus, controls the magnitude of stride (represented by the coxa angle) and self-oscillation about the roll axis (ankle angle). As a result, the ballast is effective for stabilization of walking [4].

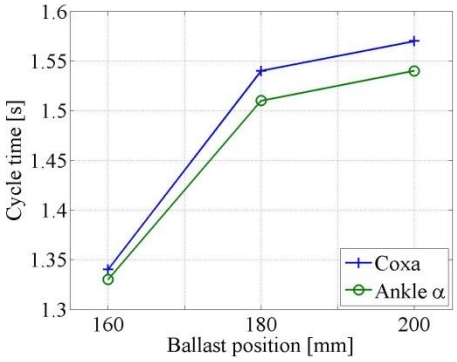

Fig.14 Ballast position vs. cycle time

Figure 14 shows cycle time of the coxa angle and the flexed angle of the ankle joint. The cycle increases when the ballast position is elevated. If the cycle time increases, then the swing leg can swing more widely. The natural frequency of the swing leg changes slightly around 3.8 rad/s (1.7 s as cycle time) as mentioned in Table 1 when the ballast position is elevated. The cycle time of the swing leg is longer than the walking cycle, and thus the magnitude of the angles as shown in Fig.13 enlarged for increase of the ballast position.

2.2 Force Sensor and ZMP

As you can see a force sensor in Fig.6, a six axes force sensor (Fig.15) is implemented so that ZMP can be measured while the walker is walking. The specification of the force sensor is shown in Table 2 and the coordinate of the ankle joint is shown in the right figure of Fig.15.

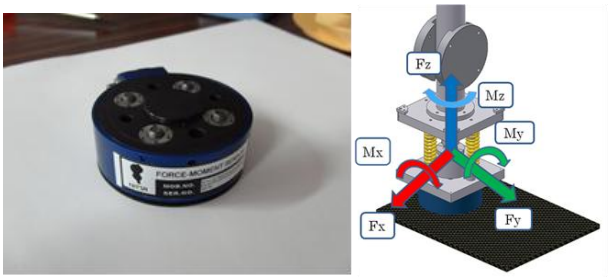

Fig.15 Force sensor and its coordinate at ankle joint

Table 2 Specification of force sensor

Force sensor	Nitta	IFS-67M25A25
F_x , F_y	F_z	M_x, M_y, M_z
100 N	200 N	7 Nm

Figures from 16 to 18 show a time evolution of moment about *x* and *y* axes, and force in the direction of vertical axis (in other words, reaction force). From Fig.16, the oscillation pattern is close to that of a typical harmonic oscillation. The roll oscillation of the gait is a kind of harmonic oscillation as a spring-mass system, and thus the oscillation dominates the stable gait, accordingly.

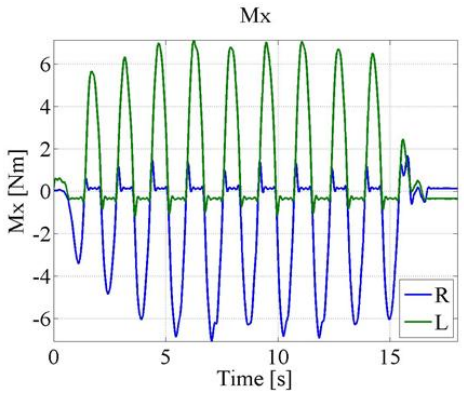

Fig.16 A time evolution of moment about *x* axis

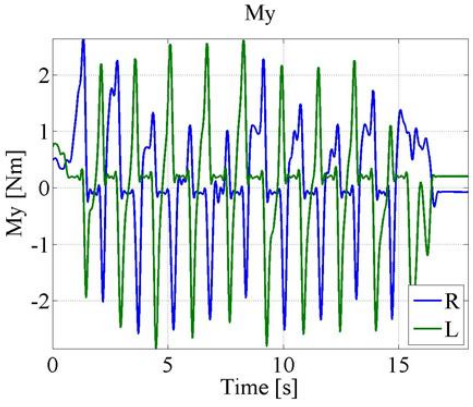

Fig.17 A time evolution of moment about *y* axis

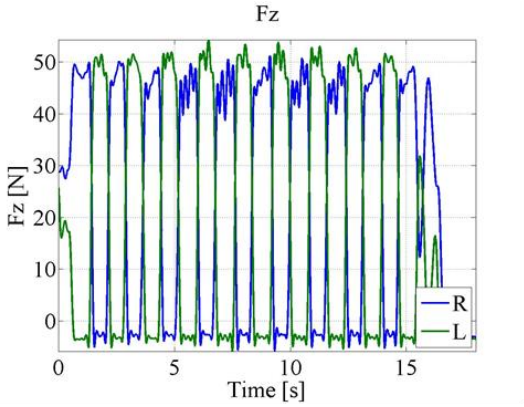

Fig.18 A time evolution of force about *z* axis

The maximum reaction force indicated about 50 N, which is little greater than the total weight of RW03 because of impact. The minimum indicated – 3 N, which is roughly corresponding to the weight of the foot. Using these data, zero moment point can be derived. Suppose that the moment about *z* axis is not considered, the position of ZMP become a point on the ground and is given by the following equation:

$$x_{zmp} = \frac{M_y}{F_z}, \qquad y_{zmp} = \frac{M_x}{F_z}$$

where, M_x (and M_y) mean moment about *x* (and *y*) axis, and F_z means force in the direction of *z* axis.

Figure 19 represents a lissajous pattern of ZMP with respect to the ballast position, 160, 180 and 200 mm from the top figure. It draws a shape of '8' bounding in two square areas representing the both soles, which means that the walker walks two steps (usually counted as one cycle of walk) in the sagittal plane while it moves one cycle in the lateral plane. The ZMP pattern is similar to that of human [9] in the sense that the pattern also draws '8', thus we can say RW03 reproduced the ZMP pattern of human in the sense of the synthetic methodology [11]. The result might be a key for explaining that emergence of human's gait is based on the 3-D PDW under physical constraints. However the pattern widens in the lateral direction. RW03 does not have knee joints, and thus the walker has to oscillate widely in the lateral direction so that the swing leg cannot scuff to the ground. The ZMP pattern is enlarged gradually when the ballast position is elevated. In case of 200 mm (the bottom figure), the pattern is slightly turbulent in the left end area. The lateral oscillation is enlarged in this case, which induces to lift the inside of the sole up.

4. CONCLUSION

In the paper, we have developed a three dimensional passive dynamic walker called RW03 and implemented a gait measurement system using unique flexible displacement sensors and a force sensor. As a result, we could observe a stable 3-D gait pattern and ZMP lissajous. Moreover the measurement system clarified the relationship between walking gait and ballast position which is effective for stabilization.

ACKNOWLEDGMENT

This research was partially supported by the Ministry of Education, Science, Sports and Culture, Grant-in-Aid (No.23760247).

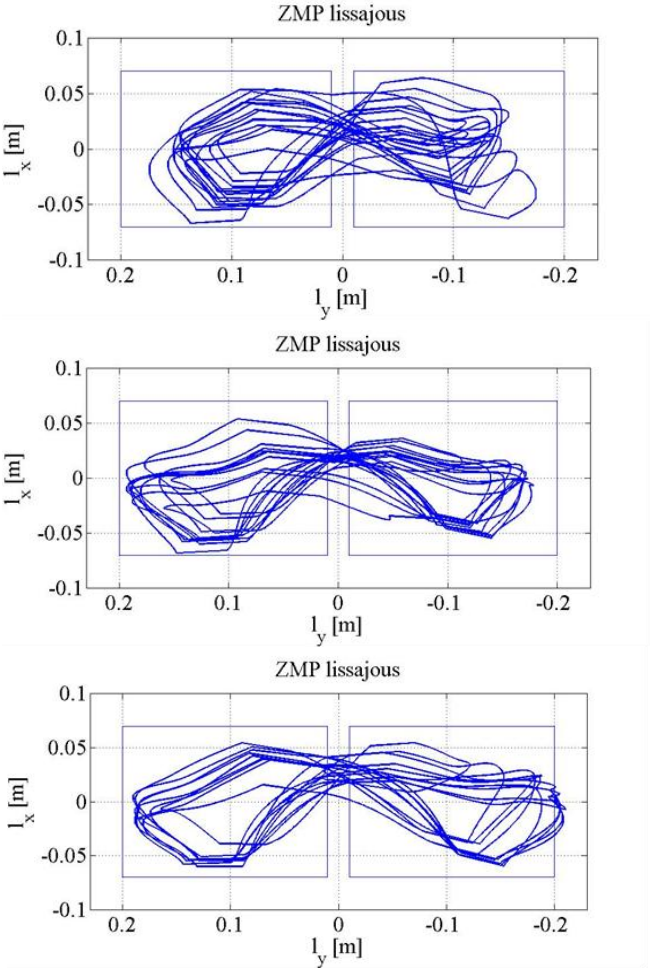

Fig.19 ZMP Lissajous with respect to the ballast position 160 mm, 180 mm, and 200 mm from the top

5. REFERENCES

[1] T. McGeer, "Passive Dynamic Walking," CSS-IS-TR, 88-2, 1988.

[2] M. Wisse, et al, "Ankle springs instead of arc-shaped feet for passive dynamic walkers," Proc. of HUMANOIDS 06, 110-16, 2006.

[3] T. Kinugasa, et al., "3D Passive Walker with Ankle Springs and Flat Feet," Journal of Robotics Society of Japan, Vol. 27, No. 10, pp. 1169-1172, 2009

[4] T. Kinugasa and K. Yoshida, "3D Passive Dynamic Walkers with Flat Feet and Ankle Springs: Experiment and Analysis For Longer and More Stable Step," Proc. of Intl. Symp. on Mobiligence, 425-430, 2009.

[5] T. Kinugasa, et al., “Experimental Analysis of 3D Passive Dynamic Walking: body’s shape, CoM and stability,” Proc. of SICE Annual Conf. 2010, 1825-1830, 2010.
[6] Collins, S. H., Wisse, M., Ruina, A., “A Three-Dimensional Passive-Dynamic Walking Robot with Two Legs and Knees,” International Journal of Robotics Research, Vol. 20, No. 2, Pages 607-615, 2001
[7] K. Narioka, K. Hosoda, "Designing synergistic walking of a whole-body humanoid driven by pneumatic artificial muscles: An empirical study", Advanced Robotics, 22(10), 1107-1123, 2008.
[8] K. Hosoda, et al., “Biped Robot Design Powered by Antagonistic Pneumatic Actuators for Multi-Modal Locomotion,” Robotics and Autonomous Systems, 56(1),46-53, 2008.
[9] I. Hamamoto, T. Akagi, et al., “Development of Flexible Displacement Sensor Using Nylon String Coated with Carbon and Its Application for McKibben Actuator,” Proc. Of SICE/ICASE Intl. Joint Conf. 2006, 1943-1946, 2006.
[10] S. Nishiyama, et al., “Estimation of zero moment point trajectory during human gait locomotion based on a three-dimensional rigid-link model,” Technical report of IECE, 101(734), 59-64, 2002.
[11] R. Pfeifer and J. Bongard, “How the body shapes the way we think: a new view of intelligence,” MIT press, 2007.